We are IntechOpen, the world's leading publisher of Open Access books Built by scientists, for scientists

6,900
Open access books available

185,000
International authors and editors

200M
Downloads

154
Countries delivered to

Our authors are among the

TOP 1%
most cited scientists

12.2%
Contributors from top 500 universities

CLARIVATE ANALYTICS
BOOK CITATION INDEX
INDEXED

WEB OF SCIENCE™

Selection of our books indexed in the Book Citation Index
in Web of Science™ Core Collection (BKCI)

Interested in publishing with us?
Contact book.department@intechopen.com

Numbers displayed above are based on latest data collected.
For more information visit www.intechopen.com

Intraoperative Human Functional Brain Mapping Using Optical Intrinsic Signal Imaging

Sameer A. Sheth, Vijay Yanamadala and Emad N. Eskandar
Department of Neurosurgery, Massachusetts General Hospital,
Harvard Medical School, Boston,
USA

1. Introduction

Functional brain mapping strives to describe the brain's organization as a mosaic of distinct regions, each of which subserves a particular function. Advances in our understanding of functional brain organization over the past decades have been propelled by the availability of increasingly sophisticated methods for assessing various aspects of neuronal activity *in vivo*. These methods can be broadly categorized as "direct" or "indirect" measures of neuronal activity (Figure 1). Direct techniques measure changes in electromagnetic fields resulting from neuronal action potentials and synaptic activity. Indirect techniques measure changes in other tissue properties that are related to neural activity. This distinction does not imply the superiority of direct over indirect techniques. Certain disadvantages of direct measures were the very motivation for the development of indirect measures. Indeed, the most widely used functional brain imaging modality currently is functional magnetic resonance imaging (fMRI), an indirect technique. A subset of indirect techniques are based on changes in blood flow subsequent to and produced by neural activity. These perfusion-dependent functional brain imaging techniques include fMRI, positron emission tomography (PET), and others. Although they are among the most commonly used methods for investigating brain function, they rely on vascular responses that are not completely understood. In this chapter, we will focus on indirect measures of brain activity, emphasizing the technique of optical intrinsic signal imaging (OISI). We discuss the physical basis of perfusion imaging and OISI, animal and human studies of OISI to date, and its potential as a powerful intraoperative functional brain mapping tool.

2. Perfusion-based functional brain imaging

In framing OISI, we first discuss the broad category of perfusion-based imaging techniques to which it belongs. Perfusion-based brain imaging techniques measure physiological events linked to neuronal activity, such as changes in metabolism or blood flow, and include positron emission tomography (PET), functional magnetic resonance imaging (fMRI), and OISI. These techniques do not measure neuronal activity *per se*; rather, they measure surrogate metabolic and vascular markers of activity. In essence, hemodynamic responses provide a map of neuronal activity spatially and temporally broadened by passage through a vascular filter. Despite their indirect nature, however, perfusion-based brain imaging

techniques are among the most commonly used, and have provided numerous important clinical and basic research insights.
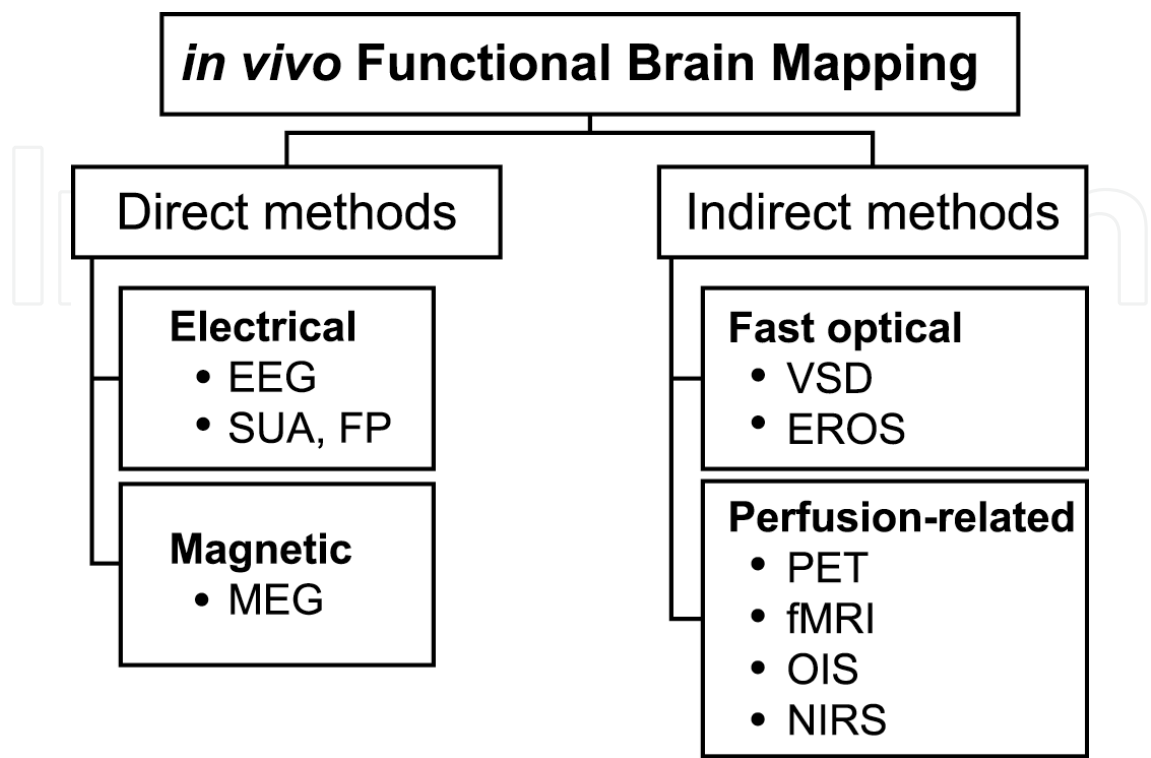
in vivo Functional Brain Mapping

Direct methods

Electrical
- EEG
- SUA, FP

Magnetic
- MEG

Indirect methods

Fast optical
- VSD
- EROS

Perfusion-related
- PET
- fMRI
- OIS
- NIRS

Fig. 1. Categorical division of *in vivo* functional brain mapping techniques. Direct methods measure electrical and magnetic field changes produced by neuronal action potentials and synaptic potentials. Electrical measures include both non-invasive techniques such as electroencephalography (EEG) and invasive techniques such as single unit activity (SUA) and field potential (FP) recording. The most common magnetic measure is magnetoencephalography (MEG). Indirect methods, on the other hand, are sensitive to other tissue changes that accompany neural activation. Structural changes produce variations in optical properties that follow the millisecond timecourse of neural events. Techniques taking advantage of these processes include voltage sensitive dye (VSD) imaging, which measures transmembrane voltage changes, and event-related optical signal (EROS) imaging, which measures optical scattering changes putatively produced by ionic movement. Indirect assessment is also possible using changes in blood flow elicited by neural activity. Hemodynamic events follow a much slower time course (several seconds), but are the most commonly used signals for functional imaging. A full appreciation of their importance for basic neurophysiology and functional imaging requires a detailed understanding of neurovascular coupling, or the relationship between neuronal activity and perfusion. PET, positron emission tomography; fMRI, functional magnetic resonance imaging; OISI, optical intrinsic signal imaging; NIRS, near-infrared spectroscopy.

3. Neurovascular coupling

Understanding the capacities and limitations of perfusion-based techniques requires an appreciation of the relationship between changes in neuronal activity and blood flow. In brief, the concept of "neurovascular coupling" describes the observation that increases in

neuronal activity trigger local increases in blood flow. Whether the perfusion response is necessary to supply an increased metabolic demand is under debate. This physiological blood flow response has several measurable properties that form the basis for the techniques described below.

The idea of neurovascular coupling dates to the late 19th century. In his tome *Principles of Psychology*, William James states,

The fluctuations of the blood-supply to the brain … followed the quickening of mental activity almost immediately. We must suppose a very delicate adjustment whereby the circulation follows the needs of the cerebral activity. Blood very likely may rush to each region of the cortex according as it is most active, but of this we know nothing. I need hardly say that the activity of the nervous matter is the primary phenomenon, and the afflux of blood its secondary consequence.

William James (1890)

James draws these conclusions from the observations of the Italian scientist Mosso, who found that cerebral blood flow was redistributed based on emotional or intellectual activity. In the same year, Roy and Sherrington published their landmark study, "On the regulation of the blood supply of the brain", in which they hypothesized a connection between neuronal activity and blood flow. Decades later in 1928, Fulton (then a neurosurgical resident under Harvey Cushing, the "father" of neurosurgery) described a clinical case involving a patient with an occipital arteriovenous malformation that produced an audible bruit when the patient engaged in visual activity [1]. This finding further strengthened the case for a causal connection between brain activity and vascular responses. Important developments occurred in the 1950s, when Kety and Sokoloff pioneered methods for measuring metabolism and blood flow changes in the whole brain using radioactive tracers [2]. Ingvar and Lassen furthered these techniques by demonstrating regional blood flow changes in response to neuronal activity in humans [3]. These methods were combined with reconstruction algorithms developed for X-ray computed tomography to give rise to PET, the first of the modern perfusion-based brain imaging techniques.

4. The hemodynamic response

Although it took over half a century to appreciate the significance of the coupling between brain activity and cerebral blood flow, the last few decades have seen a considerable advancement in our understanding of its spatiotemporal dynamics. The "hemodynamic response" refers to changes in blood flow, volume, and oxygenation generated by neuronal activation. Because perfusion-based imaging modalities are based on various aspects of the hemodynamic response, their proper interpretation requires an understanding of the characteristics of the response and its relationship to neuronal activity.

Because neurons are thought to rely on oxidative metabolism for energy production, an increase in neuronal activity leads to increased oxygen consumption, which results in extraction of oxygen from the surrounding tissue and capillaries. These events take place within the first 100-300 milliseconds following activation onset. Local oxygen extraction produces a transient increase in the relative concentration of deoxyhemoglobin (Hbr) that peaks at 0.75 – 2 seconds, depending on cortex, species, and physiological condition. Neuronal activity also triggers an increase in local cerebral blood flow (CBF), via a host of

possible mediators and incompletely understood mechanisms. The CBF response begins near the site of neural activity in small arterioles, the primary resistance vessels, and propagates retrograde to larger vessels, peaking at 2-4 seconds. The influx of oxygenated arterial blood rapidly reverses local tissue oxygenation, decreasing Hbr and increasing oxyhemoglobin (HbO_2). This oxygenation change greatly overshoots baseline, resulting in relative hyperoxygenation, peaking at 3-6 seconds. As the inflowing blood drains into the venous system, these later oxygenation changes occur in medium to large veins. If neuronal activation lasts fewer than ~4 seconds, the oxygenation changes gradually return to baseline over 10-20 seconds. If activation lasts longer, blood volume and oxygenation remain elevated for the duration of stimulation at a lower "plateau" level, and then return to baseline over several seconds after stimulus offset.

The reliance of neurons on oxidative metabolism mentioned above is a recently developed hypothesis. In the late 1980s Fox and Raichle found that relative increases in CBF were six times greater than increases in oxygen utilization [5-6]. The authors suggested that this mismatch represented uncoupling between CBF and oxygen metabolism, which they interpreted as suggesting neurons use means other than oxygen metabolism to support their energy demand. For several years, a glycoltyic mechanism for ATP production was thought to support neuronal activity. In the late 1990s, however, Buxton and Frank proposed a biophysical model of the hemodynamic response that accounted for these measurements [7-9]. They suggested that the capacity for oxygen diffusion from capillary red blood cells to neurons was reduced during the CBF response due to a decrease in capillary transit time. Blood flowing more quickly had less time to exchange oxygen with the tissue. According to this "oxygen limitation" model, a relatively larger increase in CBF was necessary to compensate for the reduced oxygen extraction, and that Fox and Raichle's data actually supported tight coupling between CBF and oxygen metabolism. This model supported the notion that oxidative metabolism accounted for the bulk of neuronal energy production. Studies using MR spectroscopy [10] and fMRI [11] provided experimental validation of this theory. In the last few years, a number of additional studies have demonstrated focal decreases in tissue oxygenation and increases in oxygen metabolism rate [12-15].

The debate over the physiology of energy metabolism has occurred almost in parallel with the debate over its implication for perfusion-based functional imaging. Some have suggested that a local increase in Hbr due to decreased tissue oxygenation would generate a transient drop in blood oxygen-level dependent (BOLD) signal ("initial dip" in fMRI parlance) [16-17]. Its close relationship to neuronal metabolism would putatively allow the initial dip to serve as a spatially accurate mapping signal for functional imaging. Although several studies have observed the dip with BOLD fMRI [18-27] and OIS spectroscopy [13, 28-31], others have not [32-36], and its existence remains somewhat controversial. Some have suggested that slightly different spatiotemporal dynamics between cerebral blood flow (CBF) and volume (CBV) could create an initial dip in BOLD signal without an increase in oxygen metabolism [9, 37]. The observation that CBV increases at least 0.5 seconds after tissue pO_2 begins to drop [15], however, makes that possibility unlikely. There now seems to be general agreement that the dip exists and is related to increased oxygen consumption. Its small size [38] and susceptibility to baseline physiological conditions [7, 32] however, jeopardize its usefulness as a mapping signal.

Although general aspects of the hemodynamic response have been fairly well characterized, relatively little is known about the mediators of the response [39]. Hypotheses explaining the molecular communication between neural activity and blood flow fall roughly into four groups [40]. According to one, byproducts of neuronal activity such as adenosine and K^+ released extracellularly cause vasodilatation in nearby blood vessels [41]. A second hypothesis promotes the role of nitric oxide (NO). In this scenario, glutamate, the predominant excitatory neurotransmitter, also acts as a mediator of neurovascular coupling. Glutamate released into the synapse binds to postsynaptic NMDA receptors and activates guanylyl cyclase to produce NO, which diffuses to neighboring blood vessels and causes vasodilatation [42]. According to a third line of thought, neuronal processes directly innervate local blood vessels and transmit vasodilatory signals through acetylcholine [43], dopamine [44], or serotonin [45]. The final and most recent argument also implicates glutamate, but highlights the role of astrocytes. Astrocytic processes ensheathing the synapse sense glutamate levels through metabotropic receptors that produce graded intracellular Ca^{2+} increases. The Ca^{2+} wave propagates to the astrocyte endfeet, which are in intimate contact with blood vessels, and triggers vasodilatation through release of various molecules including prostanoids [46].

Historically, the most commonly used perfusion-based functional brain mapping techniques have been positron emission tomography (PET) and functional magnetic resonance imaging (fMRI). The latter has experienced tremendous growth over the last ten years, eclipsing all other brain imaging techniques [47]. The demand for high-resolution imaging has also brought OISI to the forefront, along with its lower resolution but noninvasive cousin, near-infrared spectroscopy (NIRS).

Each of these imaging modalities is based on one or more aspects of the hemodynamic response. The following discussion introduces the development, basic methodology, and relative advantages and disadvantages of these techniques, with particular emphasis given to OISI and related optical techniques.

4.1 Positron emission tomography (PET)

Throughout the 1950s and 1960s, radionuclide scans were a popular tool for neurodiagnostics. The application of tomographic reconstruction techniques developed for X-ray computerized tomography (CT) to nuclear medicine heralded the rise of positron emission tomography (PET) and single photon emission computed tomography (SPECT). Introduced in 1975 by Michael Phelps [48], PET imaging was the first non-invasive (or at least minimally invasive) perfusion-based functional brain imaging modality. This technological breakthrough allowed autoradiographic measurement of metabolism [49] and blood flow [2], previously restricted to animals, to be performed in humans in the form of *in vivo* autoradiograms. The development of several biologically useful positron-emitting molecules rapidly increased the utility of PET through the late 1970s and 1980s.

PET imaging relies on the use of radioactive atoms decaying by emitting positrons, which have the same mass as electrons but a positive charge. These positron-emitting atoms are generated either through the decay of another generating element (e.g., ^{68}Ga through the decay of ^{68}Ge), or by direct production in a cyclotron (e.g., ^{15}O). Molecules containing these radioactive elements are chemically synthesized, and trace amounts injected into the subject.

The labeled molecules circulate according to their biological properties, all the while emitting positrons. The emitted positrons travel a short distance (on the order of a few mm), until they encounter their anti-particles, electrons, with which they annihilate. The annihilation produces a characteristic release of so-called synchrotron energy in the form of two 511 keV gamma rays, which travel in opposite directions, close to 180° apart.

Because of the gamma rays' high energy, PET system detectors employ elements with high atomic number and therefore high stopping power. The original detectors used thallium-doped sodium iodide (NaI[Tl]) crystals, but modern scanners use either bismuth germinate (BGO; $Bi_4Ge_3O_{12}$) or lutetium oxyorthosilicate (LSO). The detector electronics use a coincidence detection system that reduces background radiation and scatter by rejecting events that are not recorded almost simultaneously (within the preset coincidence time window) on both sides of the head. The source is assumed to exist on a line connecting the two detectors that recorded the events, and its position is determined based on the coincidence time difference. Events are recorded in this manner, and the source distribution within the brain is then calculated by solving the inverse problem using filtered back-projection or iterative approaches.

One of the advantages of PET imaging is the diversity of metabolic, hemodynamic, and biochemical processes that can be assessed using different tracers. Those that are most relevant for hemodynamic functional brain mapping are ^{15}O-labelled water ($H_2^{15}O$) and ^{18}F-labelled 2-fluoro-2-deoxy-D-glucose (^{18}FDG). $H_2^{15}O$ distributes within the circulation and collects proportionally to the regional blood flow. $H_2^{15}O$ PET is therefore the most common method for non-invasive cerebral blood flow (CBF) measurement. ^{18}FDG is actively transported into cells via glucose transporters, where it is phosphorylated in the cytoplasm and thereby sequestered intracellularly. Its 2-fluoro group prevents it from undergoing further glycolysis, so the amount accumulated within the cell indicates the rate of glucose metabolism.

More than 25 years since its introduction, PET imaging is still an important and widely used technique for clinical diagnosis and basic science research. PET offers versatility for measuring a range of physiological processes and the ability to quantify them in absolute terms. Its reliance on radiopharmaceuticals, however, limits the potential subject population and number of studies that can be performed in the same subject. In addition, PET affords rather poor spatial (several millimeters) and temporal (10s of seconds to minutes) resolution.

SPECT imaging is similar to PET in its reliance on exogenous radioisotope contrast agents. SPECT radioisotopes undergo gamma decay by emitting a single high-energy photon, as its name implies, as opposed to the two gamma rays produced by positron-electron annihilation in PET. As in PET, the contrast agents can be chosen to measure physiological responses such as CBF (e.g., ^{99m}Tc-hexamethylpropyleneamineoxime [HMPAO]). Many of the radiopharmaceuticals are commonly used in nuclear medicine and therefore do not require a cyclotron for their production. Factors such as these make SPECT imaging significantly cheaper than PET, although it suffers from even lower spatial resolution.

4.2 Functional magnetic resonance imaging (fMRI)

In 2001, fMRI surpassed EEG as the most widely used brain imaging technique, in terms of the number of published papers. Whereas EEG required 72 years to reach this level, fMRI

required only 11. This surge in popularity is a consequence of the technique's noninvasiveness and balance between sensitivity and resolution. In addition, many types of studies can be performed in clinical MRI magnets, which are increasingly available in modern health care facilities. Over the past decade, great progress has been made in improving the versatility, spatial and temporal resolution, and clinical utility of fMRI.

The phenomenon of nuclear magnetic resonance (NMR) was observed independently by Bloch and Purcell in 1945, a finding for which they were jointly awarded the Nobel Prize in Physics in 1952. NMR describes the behavior of atomic nuclei in magnetic fields. Because nuclei possess both charge and spin, they also possess an intrinsic magnetic moment. When placed in an external magnetic field ($\vec{B}_o$), nuclei align their magnetic moments parallel or anti-parallel to the field and precess about the field like a gyroscope precessing in the Earth's gravitational field. If molar quantities of spinning atoms are considered, a small fraction more tend to align parallel to $\vec{B}_o$, resulting in a net magnetization vector $\vec{M}$ parallel to $\vec{B}_o$.

Precession occurs at a characteristic frequency (the Larmor frequency, $\vec{\omega}$), which is a function of $\vec{B}_o$ and the atom's inherent properties (called its gryomagnetic constant, γ): $\vec{\omega} = \gamma \cdot \vec{B}_o$. The resonance phenomenon dictates that externally applied energy at this frequency will be transferred to the spinning atoms. Because the Larmor frequency is in the radio wave spectrum, the applied energy is called the radiofrequency (RF) pulse. The RF energy exerts a torque on $\vec{M}$, rotating it towards the transverse plane. Because the spins are still precessing, the time varying magnetic field they produce in the transverse plane induces current in a coil of wire oriented perpendicular to it. Thus transverse magnetization produces a detectable signal.

This signal decays by two processes: longitudinal (spin-lattice) and transverse (spin-spin) relaxation. The first describes the relaxation of $\vec{M}$ back to its equilibrium position, parallel to $\vec{B}_o$, and occurs with a characteristic time constant T_1. The second describes dephasing of spins due to precession at different rates, and occurs with a time constant T_2. This difference arises from spins experiencing slightly different magnetic field strengths, caused either by interactions with other spins (pure T_2 effects) or by small field inhomogeneities (T_2^* effects). Variations in the latter provide contrast for the most commonly used form of fMRI.

Imaging based on NMR involves spatially encoding the position of different spins using magnetic field gradients. Whereas NMR can be performed with any atom possessing non zero spin, imaging applications prefer spin ½ nuclei because they have only two possible energy levels. Several spin ½ atoms have been used for imaging and spectroscopy applications, including ^{3}He [50], ^{13}C [51], ^{31}P [52], and ^{129}Xe [53], but by far the most common is ^{1}H because of its abundance in the form of H_2O in biological material.

Biological imaging using NMR was developed in the late 1970s, with the first human images appearing in 1977 [54]. The word "nuclear" was dropped in the mid 1980s to avoid the associated negative connotation, in favor of the term magnetic resonance imaging (MRI). In the early 1990s, Belliveau, Rosen, and colleagues performed the first functional studies using

an injected paramagnetic contrast agent [55-57]. Contrast agents with high magnetic susceptibility produce large magnetic field gradients in the local environment, decreasing T_2^* in proportion to the amount present. Using tracer kinetic models, they compared the decrease in T_2^* weighted signal during visual activity and rest and generated a CBV weighted functional image of visual cortex [55].

At the same time, Ogawa and colleagues showed in animals that functional images could be generated without an exogenous contrast agent [58]. They took advantage of the natural difference in magnetic properties between oxy- (HbO_2) and deoxyhemoglobin (Hbr). Whereas the former is weakly diamagnetic and has little effect on magnetic fields, the latter is paramagnetic and causes local field disturbances. Hbr therefore acts as an endogenous contrast agent. The CBF response produced by functional activity reduces local Hbr content and therefore increases signal strength.

These lines of research converged in 1992, when these two groups and a third almost simultaneously demonstrated that this intrinsic oxygenation-based contrast could be used to map brain activity [59-61]. This so-called blood oxygenation level dependent (BOLD) contrast is by far the most common in fMRI studies. BOLD fMRI has spearheaded the surge in functional brain imaging over the last decade, surpassing PET due to its superior spatial and temporal resolution and avoidance of exogenous radioactive tracers.

Because it is based on blood Hbr content, BOLD fMRI temporal characteristics closely follow those of oxygenation changes, starting within 1-2 seconds of stimulation onset and peaking at 4-6 seconds. Spatially, it emphasizes venous structures because oxygenation changes are most prominent in medium to large veins. This bias tends to decrease the spatial specificity of conventional T_2^* BOLD fMRI somewhat, as veins are often millimeters away from the neuronal areas they drain. Spatial precision of a few millimeters may be sufficient for many types of cognitive studies investigating the entire brain with moderate resolution (and is certainly superior to that of PET, EEG, or MEG), but it is not sufficient for high resolution studies of columnar functional architecture.

In 1996, Malonek and Grinvald observed a small increase in Hbr before the CBF-induced hyperoxygenation [17]. They attributed this transient deoxygenation to an increase in oxidative metabolism that decreased local tissue oxygen tension before the onset of the CBF response. They suggested that imaging based on the dip could improve spatial specificity, since it was restricted to metabolically active areas.

A transient increase in Hbr would appear as a brief decrease in BOLD signal prior to the conventional positive BOLD response. Over the next several years, many investigators looked for this "initial dip" in a variety of cortices and species. It has been successfully identified in the visual cortex of cat [22-23], monkey [21], and human [18-20, 24-27], and human motor cortex [25, 27]. Although these studies identified the dip in the BOLD signal timecourse, only one study has been able to generate a map using this signal [23]. Other groups have tried, but found that the maps were not reproducible [62]. Indeed, several fMRI studies in rat somatosensory cortex have been unable to detect the dip altogether [34-36]. These discrepancies may be due to anesthesia, differences in cortical architecture, or other effects.

Alternatives to BOLD fMRI include CBF- (or perfusion-) weighted fMRI and CBV-weighted fMRI. In CBF fMRI, ^{1}H spins in arterial blood water are used as endogenous flow tracers [63-

64]. Spins outside the region of interest are labeled with an RF pulse. Labeled spins are allowed to enter the imaging region after a suitable time delay (0.5 – 2 s), where they exchange with tissue water. The amount of signal detected in the imaging slice is proportional to the flow rate into the slice. Advantages of CBF fMRI include better spatial specificity than BOLD, with less emphasis on large draining veins. In addition, whereas BOLD signals include a complex mixture of CBV, CBF, and oxygenation contributions, CBF fMRI can isolate and quantify the CBF component. This technique suffers, however, from relatively poor temporal resolution (several seconds) and lower sensitivity than BOLD [65].

The original reports of functional imaging using MRI used CBV contrast [55-57]. Current CBV fMRI studies use exogenous paramagnetic contrast agents with a long blood half-life, avoiding the need for kinetic tracer models and allowing repeated imaging. The large magnetic field disruptions introduced by the contrast agents lead to decreased T_2*-weighted signals in proportion to CBV. The temporal resolution of CBV fMRI is similar to that of BOLD fMRI, and its contrast-to-noise ratio (CNR) is much higher. The major drawback is the requirement for contrast injection, which also precludes human studies, although clinical trials are underway [66].

5. Optical intrinsic signal imaging (OISI)

Intraoperative OISI maps the brain by measuring activity-related changes in cortical light reflectance. Activity related reflectance changes were first demonstrated in nervous tissue in vitro more than 50 years ago [67] and have since been observed in vivo in rodents, cats, nonhuman primates, and humans. It is a particularly attractive brain-mapping modality because it can rapidly assess the functional activity of large cortical areas with very high spatial resolution (50–100 µm). Because of its versatility, OISI has been used to characterize numerous physiological phenomena, including neurovascular coupling [67-69], hemodynamic refractory periods [70], vasomotion [71], the organization of the visual cortex [71-73], cortical plasticity [71-76], cortical spreading depression [77], seizure [78-79], and language organization in the human brain [80]. Haglund and colleagues [81] were the first to observe optical signals in humans during seizure and cognitive tasks. Since then, the authors of studies on intraoperative OISI have described optical signal evolution in human cortex [82], the mapping of primary sensory and motor cortices [70], and the delineation of language cortices within [83] and across languages [80].

5.1 Intrinsic optical signals

OISI detects perfusion-related and metabolic signals that are coupled to neuronal activity, including hemoglobin concentration and oxygenation changes, cytochrome oxidation changes, and light scattering caused by altered blood volume, blood flow, and cell swelling [15, 17, 30, 84-86], which in turn create a functional map of the brain. Each of these different phenomena is observed and best quantified at different imaging wavelengths [30, 87]. For example, imaging at 610 nm best detects deoxyhemoglobin concentration changes because the absorbance of oxyhemoglobin is much less than that of deoxyhemoglobin at 610 nm [30]. Thus, OISI at 610 nm is analogous to BOLD fMRI [20], which capitalizes on local magnetic susceptibility changes due to differences between deoxyhemoglobin and oxyhemoglobin concentration.
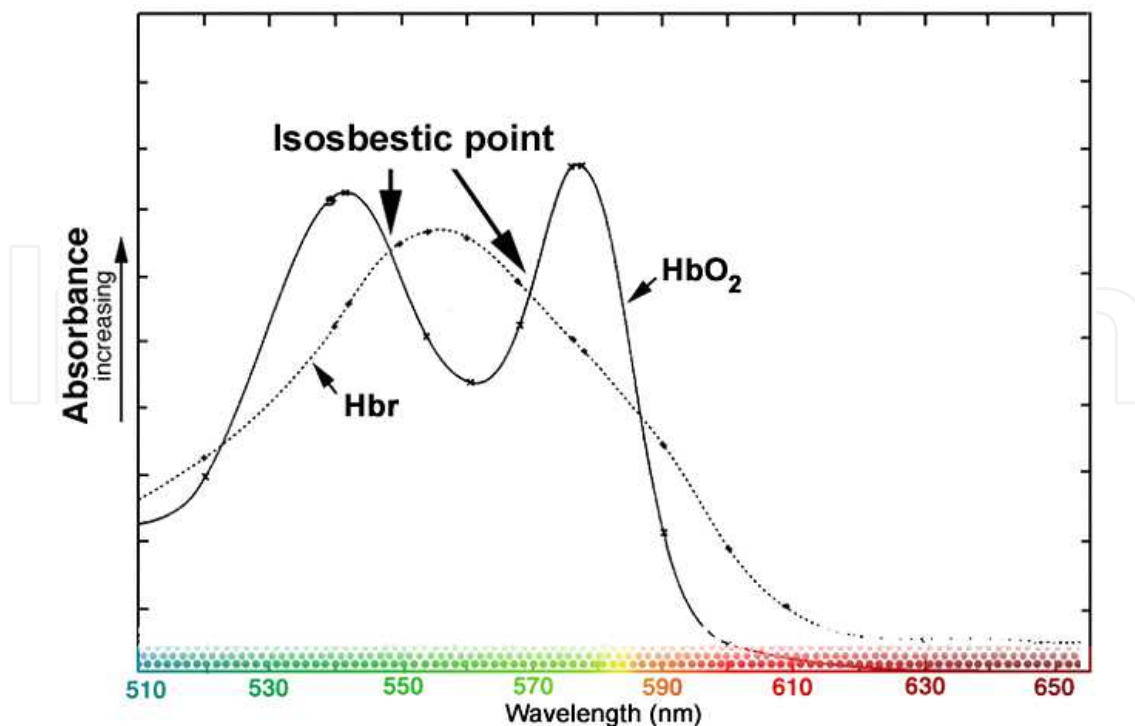
Fig. 2. Hemoglobin absorption spectrum. Optical intrinsic signal imaging (OISI) relies on changes in cortical light reflectance produced by the hemodynamic response. The most important absorber in the visible spectrum is hemoglobin (Hb). Because oxy- (HbO_2) and deoxyhemoglobin (Hbr) absorb light differentially, OISI is wavelength dependent. By selecting different imaging wavelengths, different aspects of the hemodynamic response can be assessed. Both Hb species absorb equally at isosbestic points (549, 569 nm; green light), so reflectance changes at these wavelengths emphasize changes in total Hb, a measure of blood volume. The increased absorbance of Hbr in the 605-630 nm range (red light) permits estimation of oxygenation changes by imaging in this range.

5.2 OISI mapping

Optical maps are integrated comparisons between the cortex at rest and during prescribed activity. OISI can only be performed intraoperatively in humans because it must be performed following craniotomy and dural reflection. A CCD camera is used to detect small optical changes (0.5–5%) and is mounted onto an operating microscope (Figure 3) or other support structure for imaging. The cortex is then epi-illuminated with white light, and the CCD camera captures the reflected light after it passes through a band-pass filter. Maps of functional change are calculated by comparing images during activation to images at rest [70, 80, 82-83, 89-91]. Multiple trials are averaged to increase the SNR.

Respirophasic and cardiophasic movements of the brain are significant sources of noise during imaging. Using a glass plate to immobilize the cortex [81], synchronizing image acquisition with respiration and heart rate [82] and using image registration [80-81, 83] allow for a reduction in this noise. Vascular artifacts from blood vessels are another major source of noise. Focusing 1-2 mm below the cortical surface [87] and imaging only immediately after stimulus onset [92] can minimize this artifact when the area being imaged is close to large vessels [13, 71, 93].

Commercial systems for clinical intraoperative OISI imaging are not yet available. Investigational systems can be developed from an existing operating microscope with the addition of a camera, camera controller, personal computer, and software to control image acquisition and analysis.
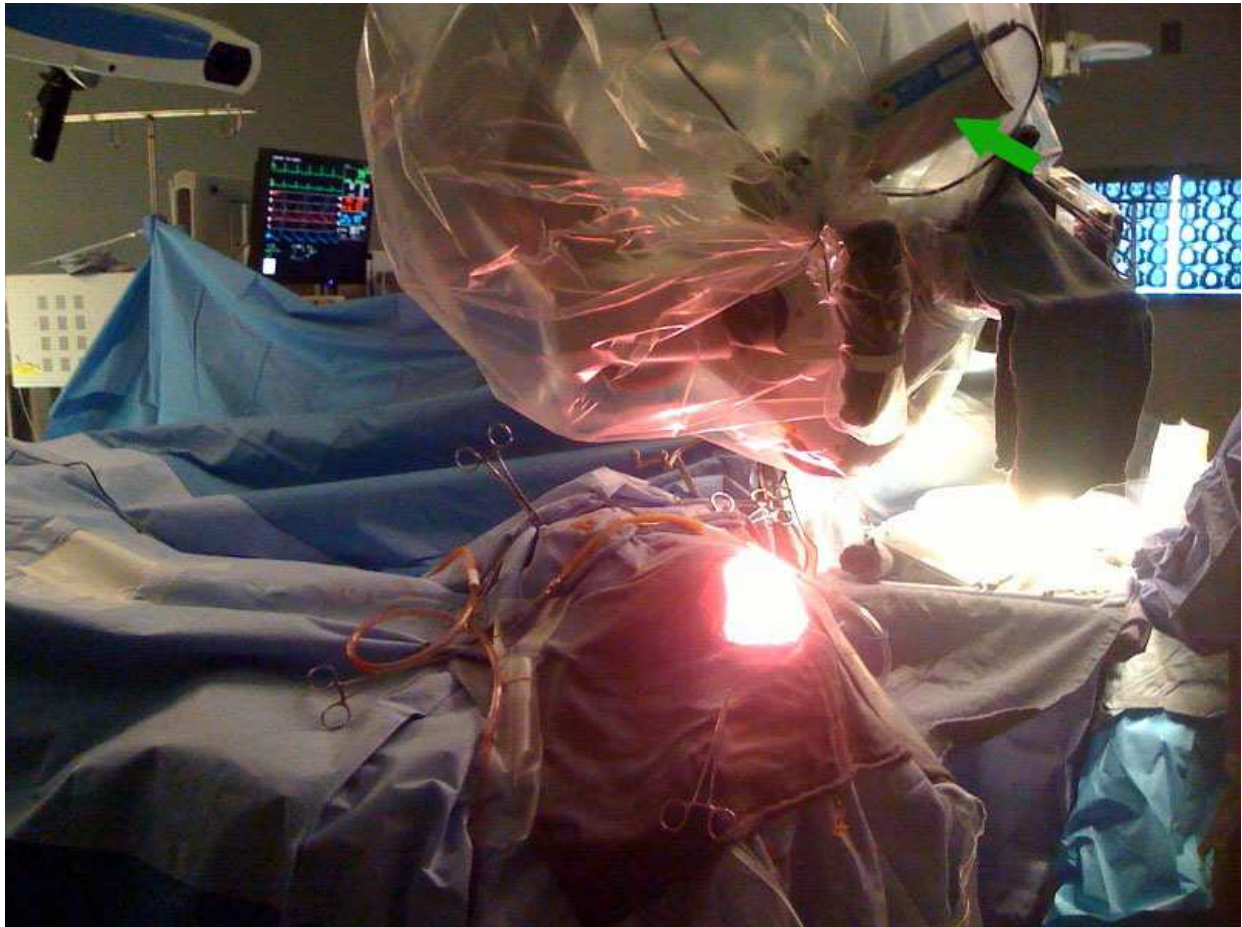

Fig. 3. Intraoperative photograph showing CCD camera mounted on operating microscope. The cortex is illuminated with white light, and the reflected light is filtered at a particular wavelength of interest. Images are captured by a very sensitive CCD camera (shown with green arrow), and reflectance changes between rest and stimulation are measured. These changes correspond to evolving aspects of the hemodynamic response generated as a consequence of underlying cortical activity.

5.3 OISI in animal models

OISI has been extensively used in animals to date and has paved the way for major breakthroughs in our understanding of the functional organization, physiology and pathophysiology of the brain [30, 68-69, 72, 74-78, 84-85, 92, 94-97]. OISI studies in animals have defined the functional topography of visual [72] and other cortices, helped elucidate the coupling between electrophysiology and perfusion-related signals, characterized the robustness of neurovascular response capacities, and described perfusion-related changes induced by pathophysiological processes such as cortical spreading depression and seizure. These studies have repeatedly demonstrated the versatility of this modality and its

numerous potential applications. The specificity of optical maps generated through OISI has been consistently confirmed in these various studies when compared to other established invasive methodologies, including single unit activity measurement [87, 95], maximum field potential measurement [96-97], and cytochrome oxidase-staining [68, 95]. OISI has also been used for mapping seizure propagation in the cortex [78] and for identifying epileptogenic foci [79].

5.4 OISI in humans

The first OISI maps of human function were created by asking the patient to engage in simple motor tasks such as tongue movement and simple language task such as visual object-naming exercises. Motor tasks demonstrated clear optical signals in the motor cortex, and language tasks demonstrated activity in both Broca and Wernicke areas [81]. Optical responses in humans typically appear within 1 second, peak between 3 and 4 seconds, and disappear by 9 seconds, similar to those observed in animal models [82, 89]. Indeed, this similar timing of optical signals across species suggests that we are indeed imaging similar phenomena, and because we have clearer physiological correlates in animals obtained through invasive methodologies, we can extrapolate that we are imaging the same neural activity. In line with this assertion, hemodynamic refractory periods originally observed in rodents were also observable in humans during OISI mapping [70]. In further corroboration, all human OISI studies to date indicate that the observed reflectance changes are spatially correlated with somatosensory evoked potential (SSEP) data. Median and ulnar nerve stimulation leads to a decrease in optical signal obtained at 610 nm in an area that colocalizes with the largest SSEPs in both somatosensory and motor cortices [82]. More importantly, OISI maps similarly colocalize with intraoperative electrocortical stimulation mapping (ESM), the current gold standard of cortical mapping [80-81, 83]. Areas that are identified by ESM as essential for a specific task consistently demonstrate optical activity [80-81, 83].

A notable phenomenon with optical signals is "vascular spread." OISI maps demonstrate signal in some surrounding areas (approximately 25%) that are not identified as essential on ESM. This has been demonstrated in both rodent models [98-100] and human intraoperative imaging. Spread may occur in part because intraoperative OISI is detecting both essential and secondary cortices whereas ESM is only detecting essential areas. Spread may also be related to imprecise physiological coupling of neuronal activity, metabolism, and perfusion. The sensitivity, specificity, positive predictive value, and negative predictive value of intraoperative OISI relative to ESM as a gold standard have not been fully quantified [101-102], and such quantification will be essential to the broadening of intraoperative OISI as a fundamental clinical tool.

OISI has also begun to provide a finer resolution of cortical mapping with regards to task specific activity. For example, OISI demonstrates differentially activated gyri during tongue movement and naming tasks, activities which require similar movements but which are otherwise distinct [81]. Median and ulnar nerve stimulation produces distinct maps within the same gyrus, possibly providing a fine resolution of somatosensory and motor activity in the cortex [82]. Distinct maps of face, thumb, and index and middle fingers have also been obtained within the same gyrus [70], and although there is some overlap between these areas, the areas of maximum optical signal are distinct for each task. Such specificity has also been observed in language areas (Broca and Wernicke areas) [83].

5.5 Advantages of intraoperative OISI mapping

The ultimate goal of intraoperative mapping is to predict when resection of a cortical area will cause functional deficits. As such, ESM is the current gold standard for intraoperative mapping because it produces reversible lesions such as would occur permanently with resection. However, ESM interpretation is complicated by the fact that cortical stimulation may disrupt remote areas via stimulation of neuronal projections [103-104], and this may lead to imprecise maps [105]. Thus, direct activation-based techniques such as OISI that rely on the detection of local neuronal activity may create a clearer picture when used in conjunction with established methods like ESM.

The spatial resolution of ESM is also one of its important drawbacks. Resection within 1 cm of essential areas identified by ESM increases the likelihood of postoperative neurological deficits [106-107]. Because of this local current spread, the resolution of this techique is relatively coarse. On the other hand, OISI offers a resolution as high as 50 to 100 μm as demonstrated by numerous studies, potentially allowing for a much finer delineation of eloquence.

Rapidity of assessment is another consideration. ESM requires the testing of several sites, at different current levels, during numerous tasks. The process requires several repetitions and is relatively quite time-consuming. Intraoperative OISI provides a faster assessment of the cortical surface, as the entire field of view can be imaged at once. This advantage is particularly important when mapping multiple tasks in an area that covers several possible functional representations.

Another advantage of OISI is its non-tactile nature, as it relies solely on light reflection. ESM requires direct contact with the brain, and the application of current to its surface. This process can precipitate abnormal electrical propagation known as after-discharge activity, which can escalate into a clinical seizure. Intraoperative seizures are not only dangerous, but also often preclude further mapping, as the brain is relatively depressed afterwards.

Furthermore, essential areas identified by ESM are consistently demonstrated by intraoperative OISI maps, suggesting that they do indeed offer a relatively high sensitivity. Thus, cortical regions not demonstrating task-related OISI activity can probably be resected without functional consequence. However, vascular spread, as previously described, may produce false-positive results in OISI maps by highlighting secondary and/or non-essential cortical areas, thus hindering our ability to produce a maximal resection. Thus, OISI may not completely replace ESM but may be used in conjunction as a complementary modality to improve the accuracy of cortical maps.

OISI can also be used in conjunction with fluorescent dyes that allow for more precise physical localization of pathological tissues such as tumors. Dyes were first used in animal studies [15, 96, 107-108] for this purpose. For example, optical imaging of an intravenously injected dye in rodents demonstrates intracranial tumors with high accuracy [107], and this has correlated well with human studies as well. Preoperative injection of 5-aminolevulinic acid, a precursor of fluorescent porphyrin, could be used to identify malignant gliomas with 85% sensitivity and 100% specificity [108]. The 5-aminolevulinic acid accumulates within the malignant tissue, where it is converted to its fluorescent derivative, which is then imaged intraoperatively using optical imaging with special optics. This is a powerful adjunctive application to optical imaging that can provide spatial information of the relationship between pathological tissue and essential cortical areas.

Importantly, like all intraoperative imaging modalities, OISI presents a distinct advantage over preoperative functional mapping (as provided by fMRI or PET) because it can correct for "brain shift" following craniotomy and dural reflection [109]. This is a non-trivial problem that confounds our ability to rely on preoperative functional mapping alone. Intraoperative OISI requires only minimal modification of the neurosurgical equipment already found in the operating room and does not impact the surgery or affect normal brain tissue as it relies solely on measuring reflected light from the brain.

5.6 Limitations of intraoperative OISI mapping

While neurovascular and neurometabolic coupling to neuronal activity appear to be consistent in numerous studies to date [15, 80, 82-83, 86-87, 95-97], the major limitation of intraoperative OISI continues to be the fact that the signal does not directly arise from neuronal activity. This becomes particularly relevant when dealing with pathological cortex, as is frequently the case during neurosurgical interventions, where the coupling may not be as tight as in normal cortex. This is a major question that remains to be elucidated and arguably can only be investigated with high-resolution intraoperative measures such as OISI.

Vascular lesions such as arteriovenous malformations (AVMs) present perhaps the most important challenge. Abnormal vascular networks may provide altered and unreliable signal in cortical areas adjacent to AVMs. While several studies have found that perfusion-related mapping signals can be detected directly adjacent to AVMs and can therefore be used reliably to predict essential language sites identified by ESM [110-112], the interpretation of results in these patients should still be approached cautiously.

Vascular spread in OISI maps is another confounder in the use of intraoperative OISI as a single modality. Indeed, using it as a lone modality may produce significant false-positive results that would prevent maximum resection of pathological and non-eloquent tissue. Until we understand this spread phenomenon better and are able to control for it, intraoperative OISI cannot replace ESM. However, it may provide an important complementary modality – for example, intraoperative OISI can be used to rapidly map cortical areas of interest with high spatial resolution, and those areas found to demonstrate optical activity can then be verified by ESM.

Another potential drawback of OISI is its limited signal-to-noise ratio (SNR). In language mapping trials, SNR values range from 5:1 to 9:1 when averaging four trials. This limited SNR can be attributed to patient head motion as well as respirophasic and cardiophasic cortical movements. While SNR can be improved by increasing the number trials that are averaged, reducing cortical movements by using a glass plate [81], or synchronizing image acquisition with respiration and pulse [82], this is still a challenge that remains to be addressed. Furthermore, increasing the number of trials elongates the time required for the procedure, a distinct disadvantage. Furthermore, unlike fMRI and PET, which afford three-dimensional maps, intraoperative OISI produces surface maps, usually to a maximum depth of 1 mm. This represents a further limitation.

As the utilization of OISI increases, we will begin to understand its strengths and weaknesses to a greater extent, potentially enabling the development of auxiliary technologies that augment these strengths or overcome these weaknesses. On the whole,

however, OISI presents important new advances that can potentially improve clinical outcomes when used in conjunction with other established modalities.

6. OIS spectroscopy

One potential shortcoming of OISI, alluded to above, is its ambiguous etiology. Studies using OISI usually report "activity" as a certain fractional change in reflectance from baseline. These reflectance changes incorporate changes in absorbance and scattering related to a number of physiological processes. Specific hemodynamic processes can be isolated to some degree by choosing appropriate wavelengths, but other contributions certainly exist.

This drawback was addressed in the late 1990s by Malonek and Grinvald [16-17]. They disambiguated the various contributions of absorbance and scattering by developing a variant of OISI known as OIS spectroscopy. In its most common form, broadband light reflected from the cortex is focused on a primary image plane containing a spectrographic slit instead of a detector. The one-dimensional column of light is then incident upon a diffraction grating that disperses the light into its constituent wavelengths along a second orthogonal axis. This two-dimensional "spatio-spectral" image is then refocused on a second image plane and captured by a camera. The x-dimension of the image represents the wavelength of light at a particular point along the slit, and the y-dimension represents vertical position. Spatio-spectral images are taken over time to capture the hemodynamic response, as in other techniques.

This approach essentially sacrifices one dimension of spatial information for an extra dimension of spectral information. The advantage gained is the ability to fit the spectra acquired over time to a model containing physiological parameters that are known to change during the hemodynamic response and affect light reflectance. Models are usually based on the Beer-Lambert law, which describes light attenuation in the presence of absorbers: $Abs = \sum_i \varepsilon_i c_i l$, where ε_i is the extinction coefficient of the ith absorber, c is the absorber concentration, and l is the pathlength through the tissue. In living tissue under normal physiological circumstances, Hbr and HbO_2 are the most important absorbers in visible wavelengths. Cytochrome oxidase also absorbs in the visible range, but its oxidation state only changes in cases of extremely low oxygen saturation. Because its absorbance is also an order of magnitude smaller than hemoglobin, it is generally not considered an important model component [71]. Early models incorporated scattering as an additive linear term: $Abs = \sum_i (\varepsilon_i c_i l) + S$, which would also capture residual errors.

Spectral data are fit to the model to extract the timecourses of the model parameters, i.e., Hbr and HbO_2. OIS spectroscopy therefore provides changes in physiological variables rather than (somewhat arbitrary) reflectance changes. This advantage allows for more direct comparison between OIS data and other modalities such as fMRI.

The results derived from OIS spectroscopy are only as valid as the model. The most important model refinements have been better consideration of wavelength dependency. The fact that different wavelengths of light penetrate biological tissue to different depths has been recognized for several years [113]. Longer wavelengths penetrate deeper into tissue and therefore travel through a longer pathlength (l in the above equations), another way of

saying that they experience more scattering. To properly account for the optical pathlength and scattering, therefore, this dependency must be taken into account.

Mayhew and colleagues performed Monte Carlo simulations to calculate the distribution of differential pathlength factors in the visible spectrum [71]. Since then, several studies have incorporated wavelength dependency into the Beer-Lambert model to more accurately simulate the behavior of light transport through highly scattering biological tissue [28, 33, 114-115]. Their results have shown that accounting for wavelength dependency is critical, especially when assessing small transients in the response such as the initial dip.

6.1 Near-infrared spectroscopy (NIRS)

In 1977 Jobsis showed that the intact human skull was not necessarily a barrier for light [116]. He found that wavelengths of light beyond the visible spectrum in the near-infrared range (~670-900 nm) can penetrate through several centimeters of skin and skull. This range is ideally situated between the strong absorption spectra of hemoglobin (<~630 nm) and water (>~950 nm), and has therefore been dubbed the "biological window" for noninvasive optical imaging [117-118].

NIRS is based on the same principles as visible range spectroscopy described above. Changes in light attenuation are fit to a modified Beer-Lambert law incorporating scattering and absorption by hemoglobin. The wavelength dependency of the pathlength must be taken into account. Differential pathlength factors can also be calculated using a Monte Carlo simulation, but another method exists in the case of NIRS. Pathlengths can be directly measured using time-resolved spectroscopy systems [113, 119]. These instruments have very fast (picosecond) detectors that are capable of measuring the time of flight of photons traveling through the head, which is directly related to the distance traveled. Alternatively, frequency domain systems can measure the phase difference between incident and remitted light [120-121].

The main difference between NIRS and visible spectroscopy is the way in which light is emitted and collected. Because the cortex is not exposed, light cannot illuminate the entire area. Instead, light is directed into the head through fiber optic guides and diffuses through the skin, skull, and cortex. A detector fiber guide is positioned a few centimeters from the emitter, and captures photons that have scattered through the head in an arc-shaped path from emitter to detector. The greater the distance between emitter and detector, the more likely it is that photons will travel through a deeper arc. On the other hand, a greater separation reduces the number of photons detected. Studies have theoretically and experimentally determined the optimal spacing (2.5-4 cm) to allow the photons to "sample" the top layers of cortex [122-123]. Because functional activation is not expected to produce changes in the skull or scalp, any differences in measured light intensity are attributed to cortical hemodynamic processes, i.e., changes in oxygenation or volume.

NIRS can be performed using broadband or laser illumination. The former situation is directly analogous to visible spectroscopy: remitted light is spectrally decomposed and captured by a camera. This approach affords excellent spectral resolution, but the emitted power per wavelength band is low. In contrast, laser diodes produce more power in a narrow wavelength band, but the number of wavelengths is limited to a few (2-4 in conventional systems), decreasing spectral resolution. Detectors for laser illumination are usually photodiodes, which are much more sensitive than CCDs.

The principle advantage of NIRS over other optical techniques is its noninvasive nature. NIRS provides information about functional oxygenation and volume changes that are directly comparable to fMRI, but the apparatus is much less costly and confining. NIRS can be performed in pediatric populations much more easily than fMRI [124], and it can be transported to the bedside for clinical evaluations [125-128]. Because NIRS signals are detected several centimeters from the cortex, however, the spatial resolution of the technique is low (~1-2 cm). Spatial coverage can be increased by using arrays of emitters and detectors, but the emitter-detector spacing must be at least 2-3 cm to allow the light to sample cortex.

Modifications to the acquisition and analysis methods allow images to be created from NIRS data [129]. In this variant, a grid of emitters and detectors is placed on the head, providing several emitter-detectors pairs. NIRS imaging, or diffuse optical tomography (DOT), is the optical analog of PET, EEG, or MEG, in that it requires measurement of surface signals and calculation of the source distribution that could have produced them. It therefore also involves solving an inverse problem, which is again poorly constrained. Recent work has shown, however, that analyzing multi-channel NIRS data with this imaging approach provides better estimates of functional changes than single-channel NIRS [129].

7. Multi-modality approaches

The brain mapping techniques described above, both direct and indirect, can be combined, such that the information gained by their combination surpasses their advantages individually. The most beneficial combinations usually involve compensating for limitations of one technique with another, or concurrently measuring different aspects of the same response to better understand its physiological basis. For example, combined OISI-fMRI studies have also contributed to our knowledge of the etiology of these signals [101, 130-131]. The recent development of a system that allows simultaneous fMRI and OIS spectroscopy [132] promises to further this endeavor. This combination has also been used to test the clinical utility of intraoperative human OISI for neurosurgical guidance by comparing intraoperative OISI maps with pre-surgical fMRI maps [101, 130-131].

8. Conclusions

A central tenet in neurosurgery is avoidance of new postoperative neurological deficit. This goal is especially challenging when operating in or near "eloquent cortex", or regions subserving known specific functions, such as sensation, motor control, or language. Given individual neuroanatomical variations, eloquent regions must be delineated at the time of surgery, within the individual patient. The conventional method for identifying eloquent cortex intraoperatively is electrical stimulation mapping (ESM), during which regions of cortex are directly stimulated with a small electrical current using a hand-held probe. However, ESM has several limitations including limited spatial resolution, lengthy protocol time which places the patient at increased anesthesia and infection risk and increases costs, and a higher risk of seizure due to direct electrical stimulation of the cortex. Intraoperative OISI can provide maps of cortical function rapidly and without contacting the brain, therefore reducing operative time and seizure likelihood. These maps will be complementary to ESM for the localization of eloquent cortex. Furthermore, these maps can

also be used for basic research, including the fine-scale determination of the functional organization of the brain. Optical imaging thus presents a powerful new avenue for the advancement of clinical neurosurgery and neuroscience research.

Although intraoperative OISI has only been used for research purposes, it has significant potential as a clinical mapping tool as well. Although it is unlikely to replace ESM, it may, if used in conjunction with conventional intraoperative mapping techniques, decrease mapping time, provide high spatial resolution cortical maps, and allow mapping of multiple tasks.

9. References

[1] Fulton, J.F., *Vasomotor and Reflex Sequelae of Unilateral Cervical and Lumbar Ramisectomy in a Case of Raynaud's Disease, with Observations on Tonus.* Ann Surg, 1928. 88(5): p. 827-41.

[2] Landau, W.M., et al., *The local circulation of the living brain; values in the unanesthetized and anesthetized cat.* Trans Am Neurol Assoc, 1955(80th Meeting): p. 125-9.

[3] Lassen, N.A., et al., *Regional Cerebral Blood Flow in Man Determined by Krypton.* Neurology, 1963. 13: p. 719-27.

[4] Bonvento, G., N. Sibson, and L. Pellerin, *Does glutamate image your thoughts?* Trends Neurosci, 2002. 25(7): p. 359-64.

[5] Fox, P.T. and M.E. Raichle, *Focal physiological uncoupling of cerebral blood flow and oxidative metabolism during somatosensory stimulation in human subjects.* Proc Natl Acad Sci U S A, 1986. 83(4): p. 1140-4.

[6] Fox, P.T., et al., *Nonoxidative glucose consumption during focal physiologic neural activity.* Science, 1988. 241(4864): p. 462-4.

[7] Buxton, R.B., *The elusive initial dip.* Neuroimage, 2001. 13(6 Pt 1): p. 953-8.

[8] Buxton, R.B. and L.R. Frank, *A model for the coupling between cerebral blood flow and oxygen metabolism during neural stimulation.* J Cereb Blood Flow Metab, 1997. 17(1): p. 64-72.

[9] Buxton, R.B., E.C. Wong, and L.R. Frank, *Dynamics of blood flow and oxygenation changes during brain activation: the balloon model.* Magn Reson Med, 1998. 39(6): p. 855-64.

[10] Hyder, F., et al., *Oxidative glucose metabolism in rat brain during single forepaw stimulation: a spatially localized 1H[13C] nuclear magnetic resonance study.* J Cereb Blood Flow Metab, 1997. 17(10): p. 1040-7.

[11] Hoge, R.D., et al., *Linear coupling between cerebral blood flow and oxygen consumption in activated human cortex.* Proc Natl Acad Sci U S A, 1999. 96(16): p. 9403-8.

[12] Ances, B.M., et al., *Dynamic changes in cerebral blood flow, O2 tension, and calculated cerebral metabolic rate of O2 during functional activation using oxygen phosphorescence quenching.* J Cereb Blood Flow Metab, 2001. 21(5): p. 511-6.

[13] Mayhew, J., et al., *Spectroscopic analysis of neural activity in brain: increased oxygen consumption following activation of barrel cortex.* Neuroimage, 2000. 12(6): p. 664-75.

[14] Thompson, J.K., M.R. Peterson, and R.D. Freeman, *Single-neuron activity and tissue oxygenation in the cerebral cortex.* Science, 2003. 299(5609): p. 1070-2.

[15] Vanzetta, I. and A. Grinvald, *Increased cortical oxidative metabolism due to sensory stimulation: implications for functional brain imaging.* Science, 1999. 286(5444): p. 1555-8.

[16] Malonek, D., et al., *Vascular imprints of neuronal activity: relationships between the dynamics of cortical blood flow, oxygenation, and volume changes following sensory stimulation.* Proc Natl Acad Sci U S A, 1997. 94(26): p. 14826-31.

[17] Malonek, D. and A. Grinvald, *Interactions between electrical activity and cortical microcirculation revealed by imaging spectroscopy: implications for functional brain mapping.* Science, 1996. 272(5261): p. 551-4.

[18] Ernst, T. and J. Hennig, *Observation of a fast response in functional MR.* Magn Reson Med, 1994. 32(1): p. 146-9.

[19] Menon, R.S., et al., *BOLD based functional MRI at 4 Tesla includes a capillary bed contribution: echo-planar imaging correlates with previous optical imaging using intrinsic signals.* Magn Reson Med, 1995. 33(3): p. 453-9.

[20] Hu, X., T.H. Le, and K. Ugurbil, *Evaluation of the early response in fMRI in individual subjects using short stimulus duration.* Magn Reson Med, 1997. 37(6): p. 877-84.

[21] Logothetis, N.K., et al., *Functional imaging of the monkey brain.* Nat Neurosci, 1999. 2(6): p. 555-62.

[22] Duong, T.Q., et al., *Spatiotemporal dynamics of the BOLD fMRI signals: toward mapping submillimeter cortical columns using the early negative response.* Magn Reson Med, 2000. 44(2): p. 231-42.

[23] Kim, D.S., T.Q. Duong, and S.G. Kim, *High-resolution mapping of iso-orientation columns by fMRI.* Nat Neurosci, 2000. 3(2): p. 164-9.

[24] Yacoub, E. and X. Hu, *Detection of the early negative response in fMRI at 1.5 Tesla.* Magn Reson Med, 1999. 41(6): p. 1088-92.

[25] Yacoub, E. and X. Hu, *Detection of the early decrease in fMRI signal in the motor area.* Magn Reson Med, 2001. 45(2): p. 184-90.

[26] Yacoub, E., et al., *Further evaluation of the initial negative response in functional magnetic resonance imaging.* Magn Reson Med, 1999. 41(3): p. 436-41.

[27] Yacoub, E., et al., *Investigation of the initial dip in fMRI at 7 Tesla.* NMR Biomed, 2001. 14(7-8): p. 408-12.

[28] Jones, M., et al., *Concurrent optical imaging spectroscopy and laser-Doppler flowmetry: the relationship between blood flow, oxygenation, and volume in rodent barrel cortex.* Neuroimage, 2001. 13(6 Pt 1): p. 1002-15.

[29] Jones, M., J. Berwick, and J. Mayhew, *Changes in blood flow, oxygenation, and volume following extended stimulation of rodent barrel cortex.* Neuroimage, 2002. 15(3): p. 474-87.

[30] Nemoto, M., et al., *Analysis of optical signals evoked by peripheral nerve stimulation in rat somatosensory cortex: dynamic changes in hemoglobin concentration and oxygenation.* J Cereb Blood Flow Metab, 1999. 19(3): p. 246-59.

[31] Shtoyerman, E., et al., *Long-term optical imaging and spectroscopy reveal mechanisms underlying the intrinsic signal and stability of cortical maps in V1 of behaving monkeys.* J Neurosci, 2000. 20(21): p. 8111-21.

[32] Lindauer, U., et al., *Neuronal activity-induced changes of local cerebral microvascular blood oxygenation in the rat: effect of systemic hyperoxia or hypoxia.* Brain Res, 2003. 975(1-2): p. 135-40.

[33] Lindauer, U., et al., *No evidence for early decrease in blood oxygenation in rat whisker cortex in response to functional activation.* Neuroimage, 2001. 13(6 Pt 1): p. 988-1001.

[34] Mandeville, J.B., et al., *Dynamic functional imaging of relative cerebral blood volume during rat forepaw stimulation.* Magn Reson Med, 1998. 39(4): p. 615-24.

[35] Marota, J.J., et al., *Investigation of the early response to rat forepaw stimulation.* Magn Reson Med, 1999. 41(2): p. 247-52.

[36] Silva, A.C., et al., *Early temporal characteristics of cerebral blood flow and deoxyhemoglobin changes during somatosensory stimulation.* J Cereb Blood Flow Metab, 2000. 20(1): p. 201-6.

[37] Hathout, G.M., B. Varjavand, and R.K. Gopi, *The early response in fMRI: a modeling approach.* Magn Reson Med, 1999. 41(3): p. 550-4.

[38] Ugurbil, K., L. Toth, and D.S. Kim, *How accurate is magnetic resonance imaging of brain function?* Trends Neurosci, 2003. 26(2): p. 108-14.

[39] Villringer, A. and U. Dirnagl, *Coupling of brain activity and cerebral blood flow: basis of functional neuroimaging.* Cerebrovasc Brain Metab Rev, 1995. 7(3): p. 240-76.

[40] Parri, R. and V. Crunelli, *An astrocyte bridge from synapse to blood flow.* Nat Neurosci, 2003. 6(1): p. 5-6.

[41] Faraci, F.M., *Regulation of the cerebral circulation by endothelium.* Pharmacol Ther, 1992. 56(1): p. 1-22.

[42] Iadecola, C., *Regulation of the cerebral microcirculation during neural activity: is nitric oxide the missing link?* Trends Neurosci, 1993. 16(6): p. 206-14.

[43] Vaucher, E. and E. Hamel, *Cholinergic basal forebrain neurons project to cortical microvessels in the rat: electron microscopic study with anterogradely transported Phaseolus vulgaris leucoagglutinin and choline acetyltransferase immunocytochemistry.* J Neurosci, 1995. 15(11): p. 7427-41.

[44] Krimer, L.S., et al., *Dopaminergic regulation of cerebral cortical microcirculation.* Nat Neurosci, 1998. 1(4): p. 286-9.

[45] Reinhard, J.F., Jr., et al., *Serotonin neurons project to small blood vessels in the brain.* Science, 1979. 206(4414): p. 85-7.

[46] Zonta, M., et al., *Neuron-to-astrocyte signaling is central to the dynamic control of brain microcirculation.* Nat Neurosci, 2003. 6(1): p. 43-50.

[47] Illes, J., M.P. Kirschen, and J.D. Gabrieli, *From neuroimaging to neuroethics.* Nat Neurosci, 2003. 6(3): p. 205.

[48] Phelps, M.E., et al., *Application of annihilation coincidence detection to transaxial reconstruction tomography.* J Nucl Med, 1975. 16(3): p. 210-24.

[49] Sokoloff, L., et al., *The [14C]deoxyglucose method for the measurement of local cerebral glucose utilization: theory, procedure, and normal values in the conscious and anesthetized albino rat.* J Neurochem, 1977. 28(5): p. 897-916.

[50] Middleton, H., et al., *MR imaging with hyperpolarized 3He gas.* Magn Reson Med, 1995. 33(2): p. 271-5.

[51] Shulman, R.G., F. Hyder, and D.L. Rothman, *Biophysical basis of brain activity: implications for neuroimaging.* Q Rev Biophys, 2002. 35(3): p. 287-325.

[52] Constantinidis, I., *MRS methodology.* Adv Neurol, 2000. 83: p. 235-46.

[53] Mair, R.W., et al., *Reduced xenon diffusion for quantitative lung study--the role of SF(6).* NMR Biomed, 2000. 13(4): p. 229-33.

[54] Damadian, R., M. Goldsmith, and L. Minkoff, *NMR in cancer: XVI. FONAR image of the live human body.* Physiol Chem Phys, 1977. 9(1): p. 97-100, 108.

[55] Belliveau, J.W., et al., *Functional mapping of the human visual cortex by magnetic resonance imaging.* Science, 1991. 254(5032): p. 716-9.

[56] Belliveau, J.W., et al., *Functional cerebral imaging by susceptibility-contrast NMR.* Magn Reson Med, 1990. 14(3): p. 538-46.

[57] Rosen, B.R., et al., *Contrast agents and cerebral hemodynamics.* Magn Reson Med, 1991. 19(2): p. 285-92.

[58] Ogawa, S., et al., *Brain magnetic resonance imaging with contrast dependent on blood oxygenation.* Proc Natl Acad Sci U S A, 1990. 87(24): p. 9868-72.

[59] Bandettini, P.A., et al., *Time course EPI of human brain function during task activation.* Magn Reson Med, 1992. 25(2): p. 390-7.

[60] Kwong, K.K., et al., *Dynamic magnetic resonance imaging of human brain activity during primary sensory stimulation.* Proc Natl Acad Sci U S A, 1992. 89(12): p. 5675-9.

[61] Ogawa, S., et al., *Intrinsic signal changes accompanying sensory stimulation: functional brain mapping with magnetic resonance imaging.* Proc Natl Acad Sci U S A, 1992. 89(13): p. 5951-5.

[62] Logothetis, N., *Can current fMRI techniques reveal the micro-architecture of cortex?* Nat Neurosci, 2000. 3(5): p. 413-4.

[63] Duong, T.Q., et al., *Localized cerebral blood flow response at submillimeter columnar resolution.* Proc Natl Acad Sci U S A, 2001. 98(19): p. 10904-9.

[64] Kim, S.G., *Quantification of relative cerebral blood flow change by flow-sensitive alternating inversion recovery (FAIR) technique: application to functional mapping.* Magn Reson Med, 1995. 34(3): p. 293-301.

[65] Kim, S.G. and K. Ugurbil, *Functional magnetic resonance imaging of the human brain.* J Neurosci Methods, 1997. 74(2): p. 229-43.

[66] Sharma, R., et al., *Safety profile of ultrasmall superparamagnetic iron oxide ferumoxtran-10: phase II clinical trial data.* J Magn Reson Imaging, 1999. 9(2): p. 291-4.

[67] Hill, D.K. and R.D. Keynes, *Opacity changes in stimulated nerve.* J Physiol, 1949. 108(3): p. 278-81.

[68] Blood, A.J., S.M. Narayan, and A.W. Toga, *Stimulus parameters influence characteristics of optical intrinsic signal responses in somatosensory cortex.* J Cereb Blood Flow Metab, 1995. 15(6): p. 1109-21.

[69] Blood, A.J. and A.W. Toga, *Optical intrinsic signal imaging responses are modulated in rodent somatosensory cortex during simultaneous whisker and forelimb stimulation.* J Cereb Blood Flow Metab, 1998. 18(9): p. 968-77.

[70] Cannestra, A.F., et al., *Topographical and temporal specificity of human intraoperative optical intrinsic signals.* Neuroreport, 1998. 9(11): p. 2557-63.

[71] Mayhew, J., et al., *Spectroscopic analysis of changes in remitted illumination: the response to increased neural activity in brain.* Neuroimage, 1999. 10(3 Pt 1): p. 304-26.

[72] Bonhoeffer, T. and A. Grinvald, *Iso-orientation domains in cat visual cortex are arranged in pinwheel-like patterns.* Nature, 1991. 353(6343): p. 429-31.

[73] Shmuel, A. and A. Grinvald, *Coexistence of linear zones and pinwheels within orientation maps in cat visual cortex.* Proc Natl Acad Sci U S A, 2000. 97(10): p. 5568-73.

[74] Dinse, H.R., et al., *Optical imaging of cat auditory cortex cochleotopic selectivity evoked by acute electrical stimulation of a multi-channel cochlear implant.* Eur J Neurosci, 1997. 9(1): p. 113-9.

[75] Dinse, H.R., et al., *Optical imaging of cat auditory cortical organization after electrical stimulation of a multichannel cochlear implant: differential effects of acute and chronic stimulation.* Am J Otol, 1997. 18(6 Suppl): p. S17-8.

[76] Polley, D.B., C.H. Chen-Bee, and R.D. Frostig, *Two directions of plasticity in the sensory-deprived adult cortex.* Neuron, 1999. 24(3): p. 623-37.

[77] O'Farrell, A.M., et al., *Characterization of optical intrinsic signals and blood volume during cortical spreading depression.* Neuroreport, 2000. 11(10): p. 2121-5.

[78] Chen, J.W., A.M. O'Farrell, and A.W. Toga, *Optical intrinsic signal imaging in a rodent seizure model.* Neurology, 2000. 55(2): p. 312-5.

[79] Schwartz, T.H. and T. Bonhoeffer, *In vivo optical mapping of epileptic foci and surround inhibition in ferret cerebral cortex.* Nat Med, 2001. 7(9): p. 1063-7.

[80] Pouratian, N., et al., *Optical imaging of bilingual cortical representations. Case report.* J Neurosurg, 2000. 93(4): p. 676-81.

[81] Haglund, M.M., G.A. Ojemann, and D.W. Hochman, *Optical imaging of epileptiform and functional activity in human cerebral cortex.* Nature, 1992. 358(6388): p. 668-71.

[82] Toga, A.W., A.F. Cannestra, and K.L. Black, *The temporal/spatial evolution of optical signals in human cortex.* Cereb Cortex, 1995. 5(6): p. 561-5.

[83] Cannestra, A.F., et al., *Temporal and topographical characterization of language cortices using intraoperative optical intrinsic signals.* Neuroimage, 2000. 12(1): p. 41-54.

[84] Frostig, R.D., et al., *Cortical functional architecture and local coupling between neuronal activity and the microcirculation revealed by in vivo high-resolution optical imaging of intrinsic signals.* Proc Natl Acad Sci U S A, 1990. 87(16): p. 6082-6.

[85] Grinvald, A., *Optical imaging of architecture and function in the living brain sheds new light on cortical mechanisms underlying visual perception.* Brain Topogr, 1992. 5(2): p. 71-5.

[86] Narayan, S.M., et al., *Functional increases in cerebral blood volume over somatosensory cortex.* J Cereb Blood Flow Metab, 1995. 15(5): p. 754-65.

[87] Hodge, C.J., Jr., et al., *Identification of functioning cortex using cortical optical imaging.* Neurosurgery, 1997. 41(5): p. 1137-44; discussion 1144-5.

[88] Grinvald, A., et al., *High-resolution optical imaging of functional brain architecture in the awake monkey.* Proc Natl Acad Sci U S A, 1991. 88(24): p. 11559-63.

[89] Cannestra, A.F., et al., *The evolution of optical signals in human and rodent cortex.* Neuroimage, 1996. 3(3 Pt 1): p. 202-8.

[90] Cannestra, A.F., et al., *Temporal spatial differences observed by functional MRI and human intraoperative optical imaging.* Cereb Cortex, 2001. 11(8): p. 773-82.

[91] Cannestra, A.F., et al., *Refractory periods observed by intrinsic signal and fluorescent dye imaging.* J Neurophysiol, 1998. 80(3): p. 1522-32.

[92] Chen-Bee, C.H., et al., *Visualizing and quantifying evoked cortical activity assessed with intrinsic signal imaging.* J Neurosci Methods, 2000. 97(2): p. 157-73.

[93] Chen-Bee, C.H., et al., *Areal extent quantification of functional representations using intrinsic signal optical imaging.* J Neurosci Methods, 1996. 68(1): p. 27-37.

[94] Fukunishi, K. and N. Murai, *Temporal coding in the guinea-pig auditory cortex as revealed by optical imaging and its pattern-time-series analysis.* Biol Cybern, 1995. 72(6): p. 463-73.

[95] Masino, S.A., et al., *Characterization of functional organization within rat barrel cortex using intrinsic signal optical imaging through a thinned skull.* Proc Natl Acad Sci U S A, 1993. 90(21): p. 9998-10002.

[96] Narayan, S.M., et al., *Imaging optical reflectance in rodent barrel and forelimb sensory cortex.* Neuroimage, 1994. 1(3): p. 181-90.

[97] Narayan, S.M., E.M. Santori, and A.W. Toga, *Mapping functional activity in rodent cortex using optical intrinsic signals.* Cereb Cortex, 1994. 4(2): p. 195-204.

[98] Chen-Bee, C.H. and R.D. Frostig, *Variability and interhemispheric asymmetry of single-whisker functional representations in rat barrel cortex.* J Neurophysiol, 1996. 76(2): p. 884-94.

[99] Godde, B., et al., *Optical imaging of rat somatosensory cortex reveals representational overlap as topographic principle.* Neuroreport, 1995. 7(1): p. 24-8.

[100] Masino, S.A. and R.D. Frostig, *Quantitative long-term imaging of the functional representation of a whisker in rat barrel cortex.* Proc Natl Acad Sci U S A, 1996. 93(10): p. 4942-7.

[101] Pouratian, N., et al., *Intraoperative optical intrinsic signal imaging: a clinical tool for functional brain mapping.* Neurosurg Focus, 2002. 13(4): p. e1.

[102] Pouratian, N., et al., *Shedding light on brain mapping: advances in human optical imaging.* Trends Neurosci, 2003. 26(5): p. 277-82.

[103] Penfield, W. and K. Welch, *The supplementary motor area of the cerebral cortex; a clinical and experimental study.* AMA Arch Neurol Psychiatry, 1951. 66(3): p. 289-317.

[104] Wilson, C.L. and J. Engel, Jr., *Electrical stimulation of the human epileptic limbic cortex.* Adv Neurol, 1993. 63: p. 103-13.

[105] Ojemann, G.A., *Functional mapping of cortical language areas in adults. Intraoperative approaches.* Adv Neurol, 1993. 63: p. 155-63.

[106] Haglund, M.M., et al., *Cortical localization of temporal lobe language sites in patients with gliomas.* Neurosurgery, 1994. 34(4): p. 567-76; discussion 576.

[107] Haglund, M.M., et al., *Enhanced optical imaging of rat gliomas and tumor margins.* Neurosurgery, 1994. 35(5): p. 930-40; discussion 940-1.

[108] Stummer, W., et al., *Intraoperative detection of malignant gliomas by 5-aminolevulinic acid-induced porphyrin fluorescence.* Neurosurgery, 1998. 42(3): p. 518-25; discussion 525-6.

[109] Maurer, C.R., Jr., et al., *Investigation of intraoperative brain deformation using a 1.5-T interventional MR system: preliminary results.* IEEE Trans Med Imaging, 1998. 17(5): p. 817-25.

[110] Baumann, S.B., et al., *Comparison of functional magnetic resonance imaging with positron emission tomography and magnetoencephalography to identify the motor cortex in a patient with an arteriovenous malformation.* J Image Guid Surg, 1995. 1(4): p. 191-7.

[111] Leblanc, R. and E. Meyer, *Functional PET scanning in the assessment of cerebral arteriovenous malformations. Case report.* J Neurosurg, 1990. 73(4): p. 615-9.

[112] Maldjian, J., et al., *Functional magnetic resonance imaging of regional brain activity in patients with intracerebral arteriovenous malformations before surgical or endovascular therapy.* J Neurosurg, 1996. 84(3): p. 477-83.

[113] Delpy, D.T., et al., *Estimation of optical pathlength through tissue from direct time of flight measurement.* Phys Med Biol, 1988. 33(12): p. 1433-42.

[114] Sato, C., M. Nemoto, and M. Tamura, *Reassessment of activity-related optical signals in somatosensory cortex by an algorithm with wavelength-dependent path length.* Jpn J Physiol, 2002. 52(3): p. 301-12.

[115] Sato, K., et al., *Intraoperative intrinsic optical imaging of neuronal activity from subdivisions of the human primary somatosensory cortex.* Cereb Cortex, 2002. 12(3): p. 269-80.

[116] Jobsis, F.F., *Noninvasive, infrared monitoring of cerebral and myocardial oxygen sufficiency and circulatory parameters.* Science, 1977. 198(4323): p. 1264-7.

[117] Cope, M. and D.T. Delpy, *System for long-term measurement of cerebral blood and tissue oxygenation on newborn infants by near infra-red transillumination.* Med Biol Eng Comput, 1988. 26(3): p. 289-94.

[118] Obrig, H. and A. Villringer, *Beyond the visible--imaging the human brain with light.* J Cereb Blood Flow Metab, 2003. 23(1): p. 1-18.

[119] Chance, B., et al., *Comparison of time-resolved and -unresolved measurements of deoxyhemoglobin in brain.* Proc Natl Acad Sci U S A, 1988. 85(14): p. 4971-5.

[120] Fantini, S., et al., *Non-invasive optical monitoring of the newborn piglet brain using continuous-wave and frequency-domain spectroscopy.* Phys Med Biol, 1999. 44(6): p. 1543-63.

[121] Tsuchiya, Y., *Photon path distribution and optical responses of turbid media: theoretical analysis based on the microscopic Beer-Lambert law.* Phys Med Biol, 2001. 46(8): p. 2067-84.

[122] Firbank, M., et al., *Experimental and theoretical comparison of NIR spectroscopy measurements of cerebral hemoglobin changes.* J Appl Physiol, 1998. 85(5): p. 1915-21.

[123] van der Zee, P., et al., *Experimentally measured optical pathlengths for the adult head, calf and forearm and the head of the newborn infant as a function of inter optode spacing.* Adv Exp Med Biol, 1992. 316: p. 143-53.

[124] Hoshi, Y. and S.J. Chen, *Regional cerebral blood flow changes associated with emotions in children.* Pediatr Neurol, 2002. 27(4): p. 275-81.

[125] Adcock, L.M., et al., *Neonatal intensive care applications of near-infrared spectroscopy.* Clin Perinatol, 1999. 26(4): p. 893-903, ix.

[126] Hopton, P., T.S. Walsh, and A. Lee, *CBF in adults using near infrared spectroscopy (NIRS): potential for bedside measurement?* Br J Anaesth, 1996. 77(1): p. 131.

[127] Sokol, D.K., et al., *Near infrared spectroscopy (NIRS) distinguishes seizure types.* Seizure, 2000. 9(5): p. 323-7.

[128] Soul, J.S. and A.J. du Plessis, *New technologies in pediatric neurology. Near-infrared spectroscopy.* Semin Pediatr Neurol, 1999. 6(2): p. 101-10.

[129] Boas, D.A., et al., *The accuracy of near infrared spectroscopy and imaging during focal changes in cerebral hemodynamics.* Neuroimage, 2001. 13(1): p. 76-90.

[130] Hess, A., et al., *New insights into the hemodynamic blood oxygenation level-dependent response through combination of functional magnetic resonance imaging and optical recording in gerbil barrel cortex.* J Neurosci, 2000. 20(9): p. 3328-38.

[131] Pouratian, N., et al., *Spatial/temporal correlation of BOLD and optical intrinsic signals in humans.* Magn Reson Med, 2002. 47(4): p. 766-76.

[132] Paley, M., et al., *Design and initial evaluation of a low-cost 3-Tesla research system for combined optical and functional MR imaging with interventional capability.* J Magn Reson Imaging, 2001. 13(1): p. 87-92.
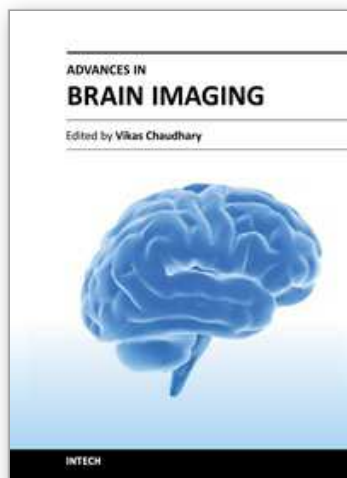
Advances in Brain Imaging
Edited by Dr. Vikas Chaudhary

Remarkable advances in medical diagnostic imaging have been made during the past few decades. The development of new imaging techniques and continuous improvements in the display of digital images have opened new horizons in the study of brain anatomy and pathology. The field of brain imaging has now become a fast-moving, demanding and exciting multidisciplinary activity. I hope that this textbook will be useful to students and clinicians in the field of neuroscience, in understanding the fundamentals of advances in brain imaging.

How to reference
In order to correctly reference this scholarly work, feel free to copy and paste the following:

INTECH
open science | open minds